Distribution Agreement

In presenting this thesis as a partial fulfillment of the requirements for a degree from Emory University, I hereby grant to Emory University and its agents the non-exclusive license to archive, make accessible, and display my thesis in whole or in part in all forms of media, now or hereafter now, including display on the World Wide Web. I understand that I may select some access restrictions as part of the online submission of this thesis. I retain all ownership rights to the copyright of the thesis. I also retain the right to use in future works (such as articles or books) all or part of this thesis.

Mariko Morimoto April 12, 2016

Synthesis and Reactivity of Novel Benzoisothiazolone Organocatalysts for Redox Condensation Reactions

By

Mariko Morimoto

Lanny S. Liebeskind, Ph.D.
Advisor

Department of Chemistry

Lanny S. Liebeskind, Ph.D.
Advisor

Jose Soria, Ph.D.
Committee Member

Chris Scarborough, Ph.D.
Committee Member

Patrick Cafferty, Ph.D.
Committee Member

2016

Synthesis and Reactivity of Novel Benzoisothiazolone Organocatalysts for Redox Condensation Reactions

By

Mariko Morimoto

Lanny S. Liebeskind, Ph.D.

Advisor

An abstract of
a thesis submitted to the Faculty of Emory College of Arts and Sciences
of Emory University in partial fulfillment
of the requirements of the degree of
Bachelor of Sciences with Honors

Department of Chemistry

2016

Abstract

Synthesis and Reactivity of Novel Benzoisothiazolone Organocatalysts for Redox Condensation Reactions
By Mariko Morimoto

In oxidation-reduction condensation reactions, loss of water can be driven stoichiometrically through the use of an organic reductant—most typically triphenylphosphine—and an organic oxidant. These traditional dehydration methods, however, are largely wasteful processes that are additionally accompanied by the use of hazardous oxidants and inseparable products. The objective of this project is to streamline redox dehydration reactions by optimizing a catalytic approach that involves the coupling of an organocatalytic benzoisothiazolone (BIT) as the oxidant and O_2 in the air as the terminal oxidant with triethylphosphite as the reductant (instead of triphenylphosphine), thus eliminating chemical waste and enhancing energy efficiency. Several novel BIT analogs retaining N-2 or N-4 pyridyl functionalization both with and without nitro-substitution on the primary aromatic ring were successfully synthesized. BIT catalyzed peptide reactions were performed open to air at room temperature and at 50ºC in acetonitrile and THF, and the carboxylic acid to amide % conversions were compared over a period of 24 h.

Synthesis and Reactivity of Novel Benzoisothiazolone Organocatalysts for Redox Condensation Reactions

By

Mariko Morimoto

Lanny S. Liebeskind, Ph.D.

Advisor

A thesis submitted to the Faculty of Emory College of Arts and Sciences
of Emory University in partial fulfillment
of the requirements of the degree of
Bachelor of Sciences with Honors

Department of Chemistry

2016

Acknowledgements

I would firstly like to thank Dr. Liebeskind for his mentorship and guidance on all aspects of this project. His encouragement and tremendous support over the years were crucial in allowing me to realize my passion for chemistry and my desire to pursue a lifelong career in this field. I thank Dr. Pavankumar Gangireddy for teaching me all of the skills that I needed in the lab, and for consistently providing me with constructive feedback. I thank Dr. Soria for his input and advice as my major advisor, and for going above and beyond this role. I would like to thank Dr. Scarborough and Dr. Cafferty for being a part of my thesis core committee, and all of the other members of the Liebeskind lab for sharing their data and insights with me. I also thank Dr. Fred Strobel from the Emory University Mass Spec Facility and Dr. John Basca from the Emory University X-ray Crystallography Center for their technical support in obtaining mass and crystal data. Finally, I thank my parents, grandparents, and friends for their constant encouragement and support.

Table of Contents

Introduction

In condensation bond forming reactions, loss of water drives the construction of a bond between hydroxyl derivatives and N-, C-, or O- moieties, as shown in Scheme 1. The sheer adaptability of this reaction is evidenced by its ability to facilitate a wide variety of bond formation, thus constituting one of the most crucial transformations in organic synthesis and biological processes.

Scheme 1. Dehydrative bond forming reactions can be acylative, alkylative, or arylative

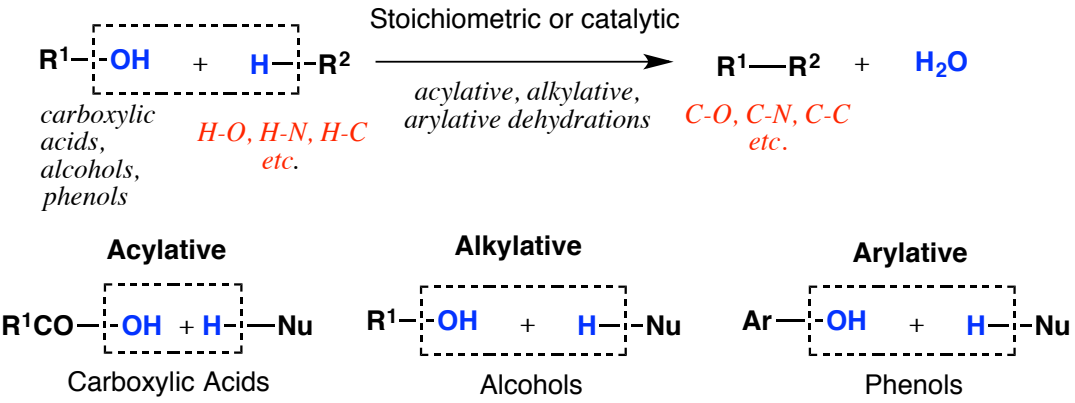

Traditionally, the elimination of water was driven in a stoichiometric fashion, through the use of stoichiometric amounts of reagents to activate the hydroxyl moiety. One specific subset of these stoichiometric activations uses an oxidation-reduction condensation process.[1] The oxidation-reduction condensation process involves the use of a weak organic reductant as an acceptor for the 2[H] of H_2O combined with an organic oxidant that functions as an acceptor for [O]. The characteristic mild and neutral reaction conditions as well as the lack of acidic or basic promoters have enabled extensive application of this reaction.[2-6] Pathways involving acylation and peptide forming reactions using carboxylic acids have been disclosed by Mukaiyama[2,7,8] and further developed to include alkylation reactions using alcohols by Mitsunobu in the well-established Mitsunobu reaction.[3,6,9,10] These dehydration methods, however, are largely wasteful processes that are accompanied by the use of hazardous oxidants and inseparable products.[11] A common oxidant in alkylation processes is diethyl

azodicarboxylate (DEAD), which possesses high toxicity and shock sensitivity as well as generates hydrazine waste of which removal is difficult.[11,12] Triphenylphosphine (TPP), the common reductant in acylation, peptide, and alkylation processes, is ultimately oxidized to triphenylphosphine oxide (TPPO), a highly soluble and chromatographically difficult to remove compound.[11] Furthermore, the stoichiometric nature of these dehydration methods inevitably raises the issue of poor atom economy, constituting a largely resource inefficient and environmentally unfavorable reaction.

In general, the stoichiometric oxidation-reduction condensation pathways can be enhanced, both in terms of atom economy and environmental sustainability, by converting to a catalytic cycle. To this end, a feasible catalytic cycle would involve regenerative organocatalytic oxidants and reductants, coupled with earth-abundant and cost efficient terminal oxidants and reductants. Though catalytic approaches to acylative redox condensation reactions have yet to be described in the literature, approaches to an organocatalytic alkylative (Mitsunobu) reactions have been taken. According to Toy, successful Mitsunobu esterification of 4-nitrobenzoic acid was accomplished using 10 mol% of DEAD as a catalytic oxidant and $PhI(OAc)_2$ as the terminal oxidant, with PPh_3 as the reductant.[13] Taniguchi further improved upon this organocatalytic Mitsunobu system primarily by altering the re-oxidant; an iron phthalocyanine organocatalyst was utilized in conjunction with atmospheric air as the terminal oxidant.[14] The successful catalytic usage of iron phthalocyanine as an alternative to DEAD also demonstrates progress towards a greener redox condensation catalytic cycle.

Thus, we are able to identify several requirements to make the existing redox condensation catalytic cycle greener for both acylative and alkylative transformations. The organic oxidant and reductant involved in the redox process must be safe, both in terms of toxicity and sensitivity to environmental conditions. Ideally, both oxidant and reductant

would be organocatalytic and regenerative, which would entirely eliminate the issue of waste removal from the final product. However, in the case that either oxidant or reductant is used stoichiometrically, the reagents must be inexpensive, commercially available, and easily removable as reaction byproducts. In an organocatalytic system, the terminal oxidant (and terminal reductant for a fully catalytic system) should be earth-abundant and cost efficient in order to fulfill the requirement of being environmentally sustainable.

In the past, Mukaiyama has utilized sulfenamides as a stoichiometric organic oxidant coupled with triphenylphosphine as the reductant in the successful redox condensation synthesis of peptide bonds between carboxylic acids and amines.[15] Seeing potential in this use of sulfenamides as an organocatalytic oxidant for acylative bond formations, we have focused on a specific heterocyclic subset of sulfenamides; namely, benzoisothiazolones (BITs) as shown in Fig.1.

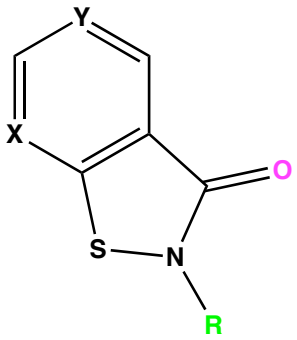

Figure 1. Prototype of benzoisothiazolone organocatalysts (X, Y, and R are variable substituents and functionalizations)

The S-N bond present in BITs can be optimized in reactivity by adjusting both electronic and substituent effects, which can be achieved by altering the substituents and functionalization on the primary aromatic ring as well as on the N. The BIT catalytic cycle facilitating a simple acylative bond formation is described in Scheme 2.

The BIT undergoes a transformation to an S-acyl-2-mercaptobenzoic acid amide compound and then to a fully reduced 2-mercaptobenzoic acid amide compound, which is then easily oxidized back to the BIT through the use of a copper catalyst.[16,17] In this regeneration of the organocatalyst, O_2 in the air serves as the terminal oxidant, resulting in the formation of water as the byproduct. Aerobic BIT regeneration has been observed to proceed via Cu-ligand coordination and disulfide formation prior to S-N closure.[18] A variety of CuI-ligand compounds were screened for catalytic efficiency in a system of 1.0 equiv p-toluic acid, 1.2 equiv benzylamine, 1.5 equiv triethylphosphite, and 20 mol% of 5-nitro-N-isopropyl-benzoisothiazolone in DMF with 4 Å molecular sieves at 50 ºC, open to dry air. $CuI_2(NMI)_4$ [19] demonstrated the best performance and was used as the oxidation catalyst for all subsequent reactions.

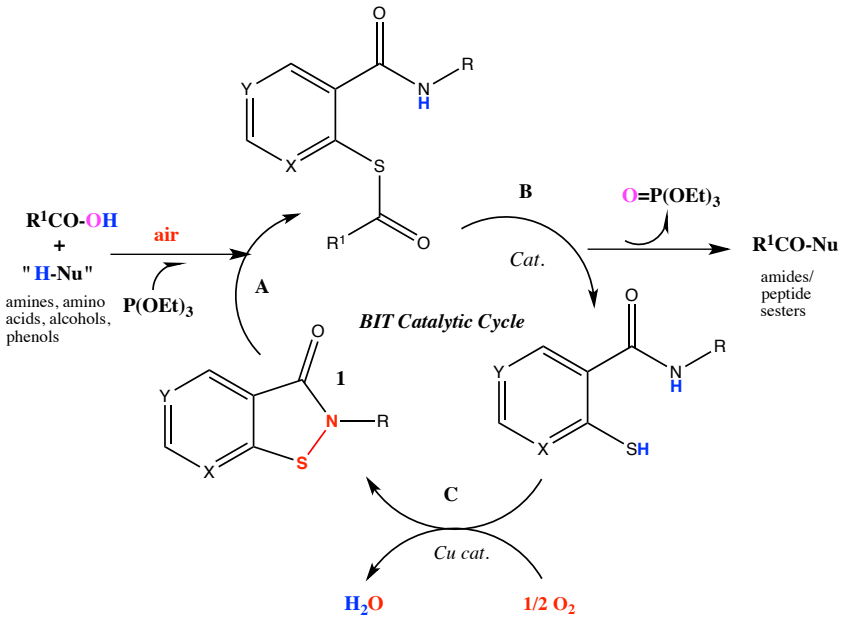

Scheme 2. Presumed aerobic catalytic cycle of BIT in acylative bond formation

As shown in Scheme 2, we have substituted stoichiometric triethylphosphite in the place of triorganophosphine as the terminal reductant. Triethylphosphite was a reasonable candidate as a terminal reductant due to its commercial availability, low cost, and low molecular weight. The primary advantage of utilizing triethylphosphite, however, comes

from its transformation to triethylphosphate as its fully oxidized byproduct, which is easy to remove post-reaction.

Mechanistic Complexities

The mechanism of catalysis can be altered depending on the N-substituent of the BIT and the solvent that the catalytic cycle takes place in. The following mechanistic pathways are presumed to be opposite ends of a continuous spectrum, with catalytic systems with solvents of intermediate polarity and BITs of different N-substituents falling somewhere in between the two extremes.

The Protonation-facilitated Thioester Pathway:

The protonation-facilitated thioester pathway is presumed to be the primary organicatalytic pathway for N-alkyl substituted BITs in non-polar solvents. As demonstrated in Scheme 3, the pathway commences with a proton transfer from the carboxylic acid to the amide, which facilitates the nucleophilic attack of the phosphate and cleavage of the S-N bond of the heterocycle.

Scheme 3. Proton-facilitated thioester pathway for N-alkyl BITs in non-polar solvents

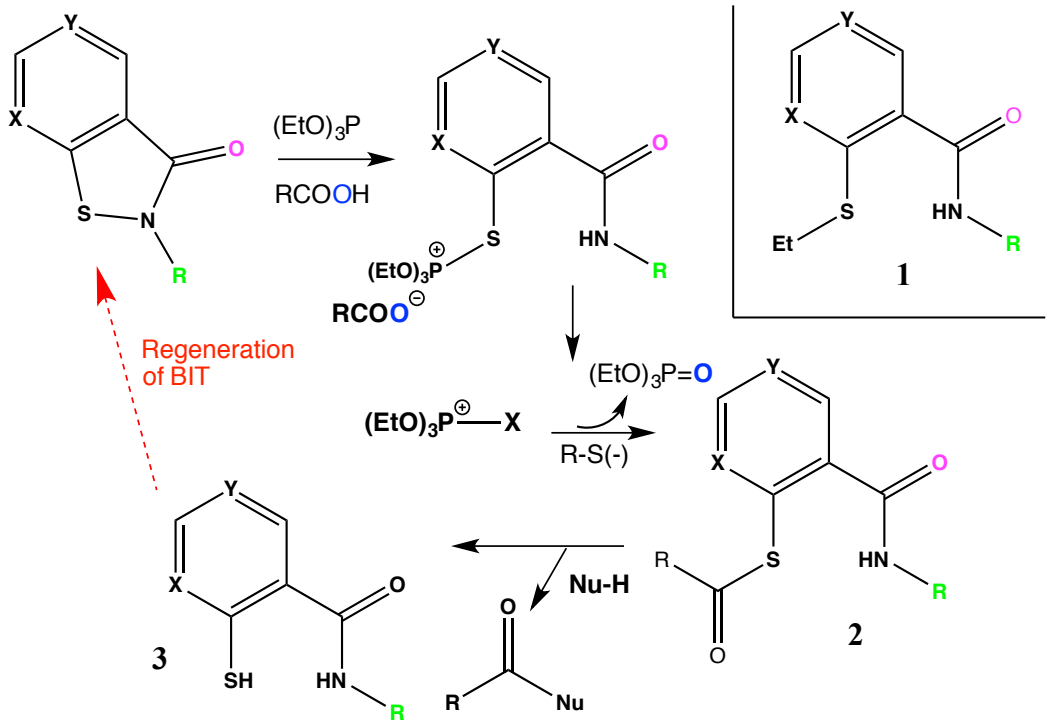

This bond-breakage event in the presence of a nucleophilic carboxylic acid ion results in the generation of an electrophilic ethoxyphosphonium ion. It is important to note that this electrophile can lead to the unproductive generation of the S-ethylation product (**1**), which is catalytically inactive and thus leads to a lower catalytic turnover rate. The final peptide product is formed from the S-acyl 2-mercaptobenzoic acid amide (**2**), and the remaining fully reduced 2-mercaptobenzoic acid amide (**3**) is then regenerated via the disulfide to the original BIT.

The Direct Deoxygenation Pathway

In unpublished results of Dr. Pavankumar Gangireddy of the Liebeskind Laboratory, a direct deoxygenation pathway was discovered as an alternative mechanistic pathway for N-aryl substituted BITs in polar solvents.[18] The exact mechanistic details are less obvious for this pathway than those of the protonation facilitated thioester pathway, particularly in the step immediately before the formation of the final peptide product. The steps in the direct deoxygenation pathway are demonstrated in Scheme 4, which begins with the elimination of oxygen from the BIT, and oxidation of the triethylphosphite to triethylphosphate.

Scheme 4. The direct deoxygenation pathway for N-aryl BITs in polar solvents

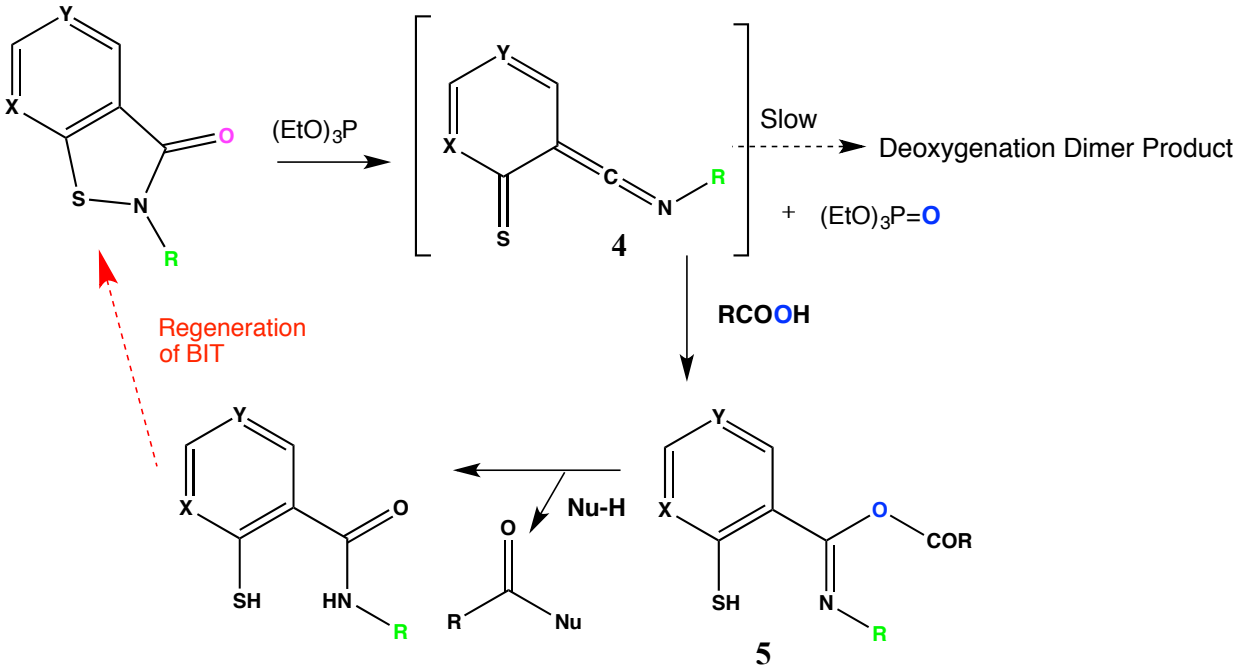

The imino cyclohexadiene-thione (**4**) intermediate is anticipated to undergo two possible reaction pathways: in unpublished results of Dr. Pavankumar Gangireddy it has been shown to dimerize to imine analogs of dibenzo dithiocine compounds in the absence of the carboxylic acid. Alternatively, the highly reactive ketene-imine functional group could also capture the carboxylic acid to generate the mixed imino anhydride (**5**) shown in Scheme 4, which could participate in the catalytic amidation chemistry. After the formation of the final amide/peptide product, the BIT would be regenerated in the same way as in the protonation facilitated thioester pathway. Though the two mechanisms are outlined separately, any combination of the two presumed pathways can be expected to take place simultaneously.

Results and Discussion

I. Synthesis of Benzoisothiazolone Organocatalysts:

Synthetic pathways for three novel BITs, 5-nitro-2-(pyridin-2-yl)benzo[d]isothiazol-3(2H)-one, 5-nitro-2-(pyridin-4-yl)benzo[d]isothiazol-3(2H)-one, and 2-(pyridin-4-yl)benzo[*d*]isothiazol-3(2*H*)-one, were developed and optimized to afford yields over 30% for each compound.

Synthesis of 5-nitro-2-(pyridin-2-yl)benzo[d]isothiazol-3(2H)-one:

The synthetic approach to **13** began with an initial attempt to synthesize a singly acylated S-tert-butyl compound (**8**), the precursor from which the S-N bond can be formed to close the heterocycle (Scheme 5).

Scheme 5. Initial synthesis attempt for 2-(*tert*-butylthio)-5-nitro-*N*-(pyridin-2-yl)benzamide

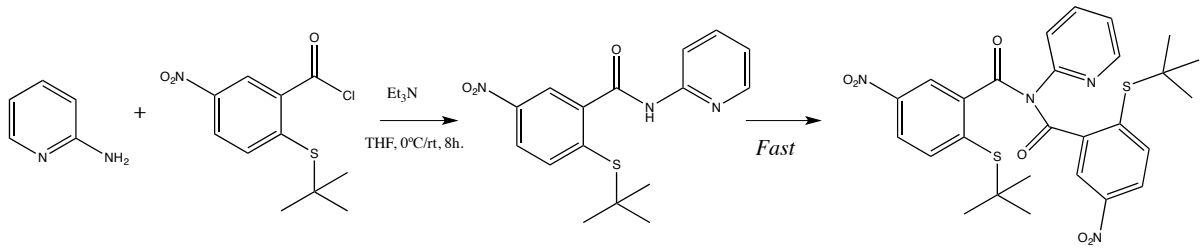

6 **7** **8** **9**

In this attempt, pyridin-2-amine (**6**) and an acid chloride (**7**) were combined in the presence of a base in a simple substitution reaction. The base would abstract a proton from the amine, enabling it to become a better nucleophile in the subsequent attack on the electrophilic carbon of the acid chloride. The yields of **8**, however, were consistently low, and spectral data indicated the presence of the doubly acylated major product, **9**. In an attempt to prevent abstraction of the acidic NH hydrogen on **8**, pyridine was used in the place of Et_3N in a subsequent reaction. Despite using a weaker base, the doubly acylated product persisted and yields of **8** remained too low for the reaction to be viable. From these initial attempts, it was concluded that the NH hydrogen on **8** was too acidic in the presence of a base, and an alternative method was necessary in the synthesis of **8**.

The synthesis of **8** was accomplished through the addition of a Boc-protecting group on the amine (**6**), as shown in Scheme 6. The Boc-protected amine was then reacted with an acid chloride (**7**), and double acylation was prevented by avoiding the formation of the acidic NH after the first deprotonation of **10**. The use of the Boc-protected amine was also advantageous in that the deprotection of **11** could be accomplished quite effortlessly by the addition of TFA, generating carbon dioxide and a nucleophile trapped *t*-butyl cation as byproducts. The reaction consistently produced a nearly 100% yield of the pure singly-acylated product (**8**).

The closing of the S-N heterocycle was accomplished through the oxidation of **8** to **12** using mCPBA as the oxidant and monitored by TLC to avoid over-oxidation. The final BIT compound (**13**) was attained by simply heating the oxidation product (**12**) in toluene. The TLC immediately after the work up for **12** demonstrated two spots, and upon heating, the spots gradually merged into one, suggesting that **12** was already converting to **13**—the heating during work up of **12** was sufficient to already initiate the conversion. Total conversion of **12** to **13** was completed in less than 20 minutes of continuous heating and

monitoring with TLC, as confirmed by spectral data and the formation of an insoluble, neon-green compound.

Scheme 6. Synthesis pathway of 5-nitro-2-(pyridin-2-yl)benzo[d]isothiazol-3(2H)-one (**13**)

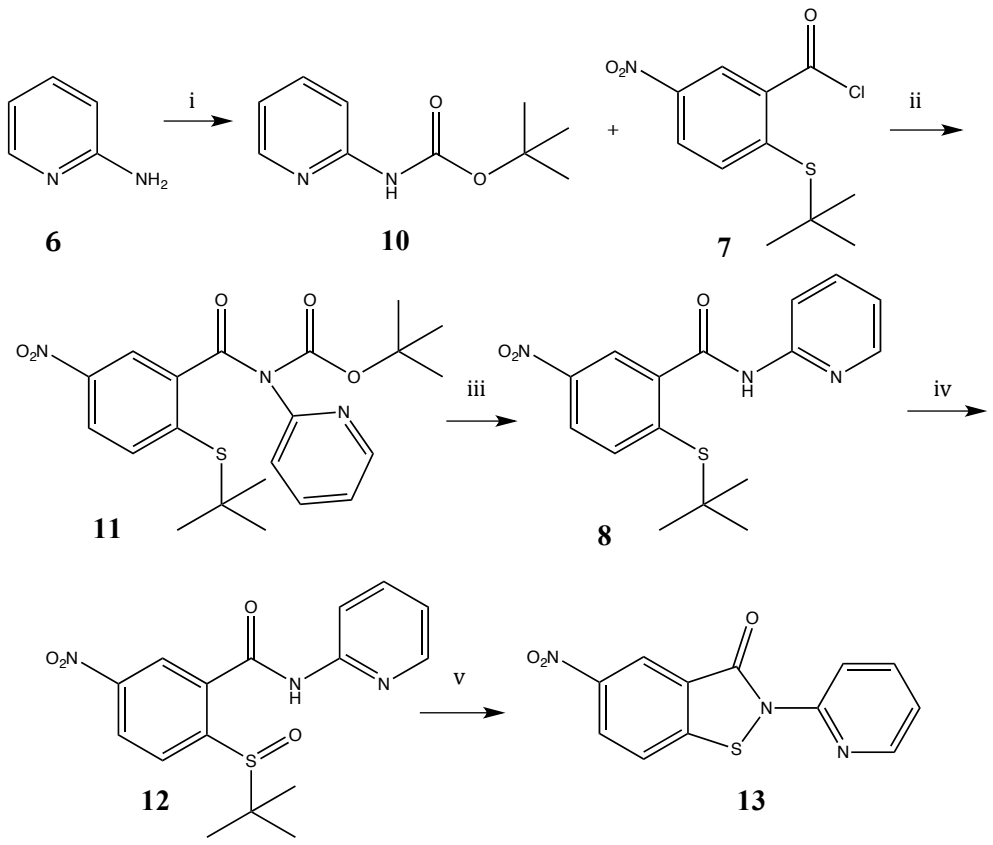

i. Boc anhydride, *tert*-butyl alcohol, rt, 24 h; ii. Et_3N, THF, rt, 8 h; iii. TFA, DCM, 0 ºC/rt, 8 h; iv. mCPBA, DCM, 0 ºC, 20 min; v. toluene, Δ

Other conventional protocols to form the S-N bond were also experimentally tested, including the addition of DMSO and TMSCl to **8**, as well as placing **12** under a pyridine/toluene reflux for 8 h. The yields, however, were significantly lower than that of v. in Scheme 6, indicating the current method to be the most efficient in terms of time and yield.

I. b.) Synthesis of 5-nitro-2-(pyridin-4-yl)benzo[d]isothiazol-3(2H)-one:

The initial attempt in the synthesis of 5-nitro-2-(pyridin-4-yl)benzo[d]isothiazol-3(2H)-one **(19)** consisted of replacing pyridin-2-amine (**6)** with pyridine-4-amine (**14)** and following the synthetic pathway outlined in Scheme 6. Pyridin-4-amine was reacted with Boc-anhydride and the pyridine-4-amine equivalent of Boc-protected **10** was synthesized

(**15**). As shown in Scheme 7, Boc-protected **15** was reacted with the acid chloride (**7**) in an attempt to synthesize an isomer of **11**.

Scheme 7. Initial synthesis attempt of 5-nitro-2-(pyridin-4-yl)benzo[d]isothiazol-3(2H)-one

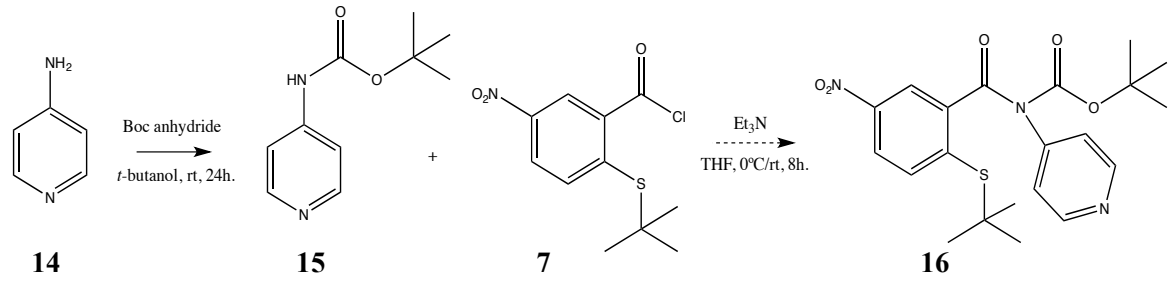

14 **15** **7** **16**

The resulting yield, however, was very low as demonstrated by the crude ^{1}H NMR spectrum. Attributing the low yield to a decrease in acidity of the NH in **15** in comparison to that of **10**, DMAP was utilized in the place of Et_3N to facilitate the deprotonation of **15**. This attempt too resulted in equally low yields, possibly implying the high electronic significance of the proximity of the pyridine N in determining both the acidity and subsequent reactivity of the amine (**15**). From these results, we reverted back to a direct approach in which the acid chloride (**7**) was added drop-wise to a solution of excess amine (**14**), as shown in Scheme 8.

Scheme 8. Synthesis pathway for 5-nitro-2-(pyridin-4-yl)benzo[d]isothiazol-3(2H)-one (**19**)

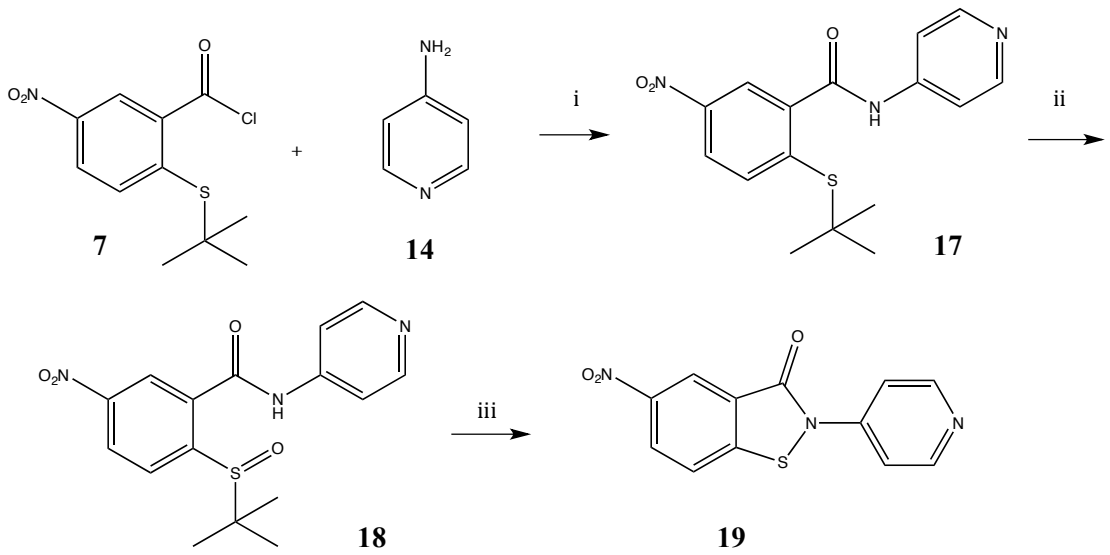

7 **14** **17** **18** **19**

i. 0.1 M THF, 0 ºC/rt, 8 h; ii. mCPBA, DCM, 0 ºC, 20 min; iii. toluene, Δ

In addition to using an excess of amine, the lack of base as well and lower reactivity of **14** were presumed to be factors contributing to a high yield (>75%) of **17** instead of the diacylation product. Compounds **18** and **19** were then synthesized using the same techniques as outlined in Scheme 6 (**12** and **13**).

I. c.) Synthesis of 2-(pyridin-4-yl)benzo[d]isothiazol-3(2H)-one:

The synthesis of **21** was accomplished through the reaction between the disulfide of the acid chloride (**20**) and an excess of the amine (**14**). The resulting disulfide amide would then disproportionate and results in the generation of an equivalent of **21**, as an amide N undergoes a nucleophilic attack on the closest S, cleaving the disulfide bond.

Scheme 9. Synthesis pathway for 2-(pyridin-4-yl)benzo[d]isothiazol-3(2H)-one (**21**)

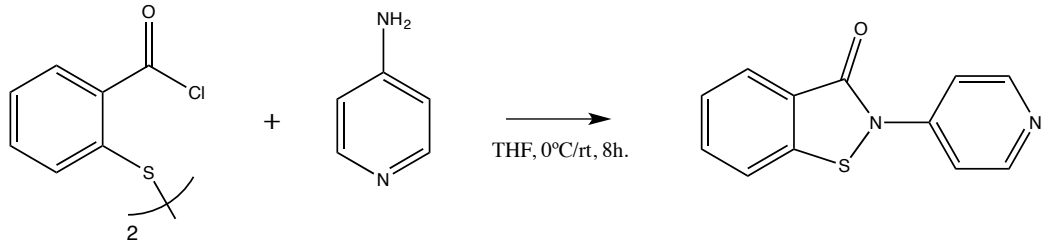

20 **14** **21**

II. Catalytic Studies of the Benzoisothiazolone Organocatalysts

This catalytic study screened the relative performances of five different BITs (**13**, **19**, **21**, **22**, **23**[20]) in catalyzing a model amide bond formation reaction at room temperature and 50 ºC. As shown in Scheme 10, 1.0 equiv. of *p*-toluic acid, 1.1 equiv of benzylamine, and 1.5 equiv triethylphosphite were kept under dry air in the presence of 0.2 equiv of each organocatalyst and 0.1 equiv of the copper regeneration catalyst. 4 Å molecular sieves were utilized as a means of maintaining low moisture levels throughout the reaction. The amide conversion % was periodically measured by gas chromatography over a span of 24 hours using 1 equiv of 1,3,5 tri-*tert*-butylbenzene added to the reaction as an inert, internal reference compound.

Scheme 10. Model amide bond synthesis reaction in BIT organocatalyst screening

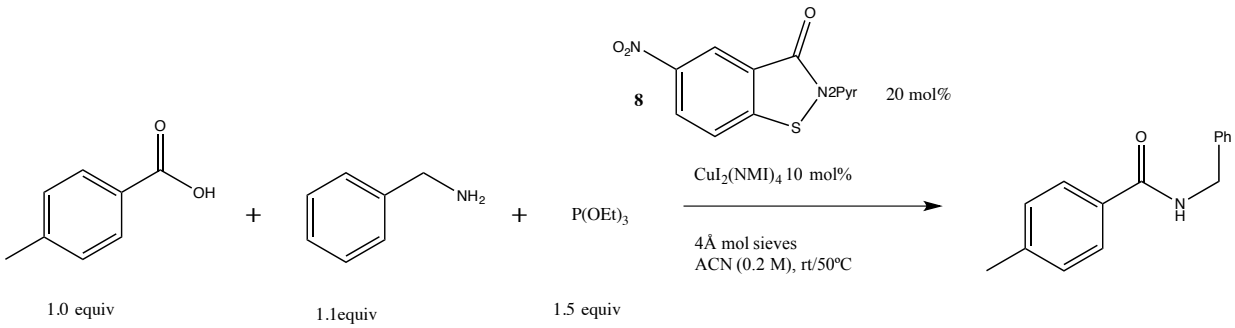

As shown in Fig. 2, the BIT organocatalysts were screened in acetonitrile at room temperature (30 ºC) over a period of 24 h.

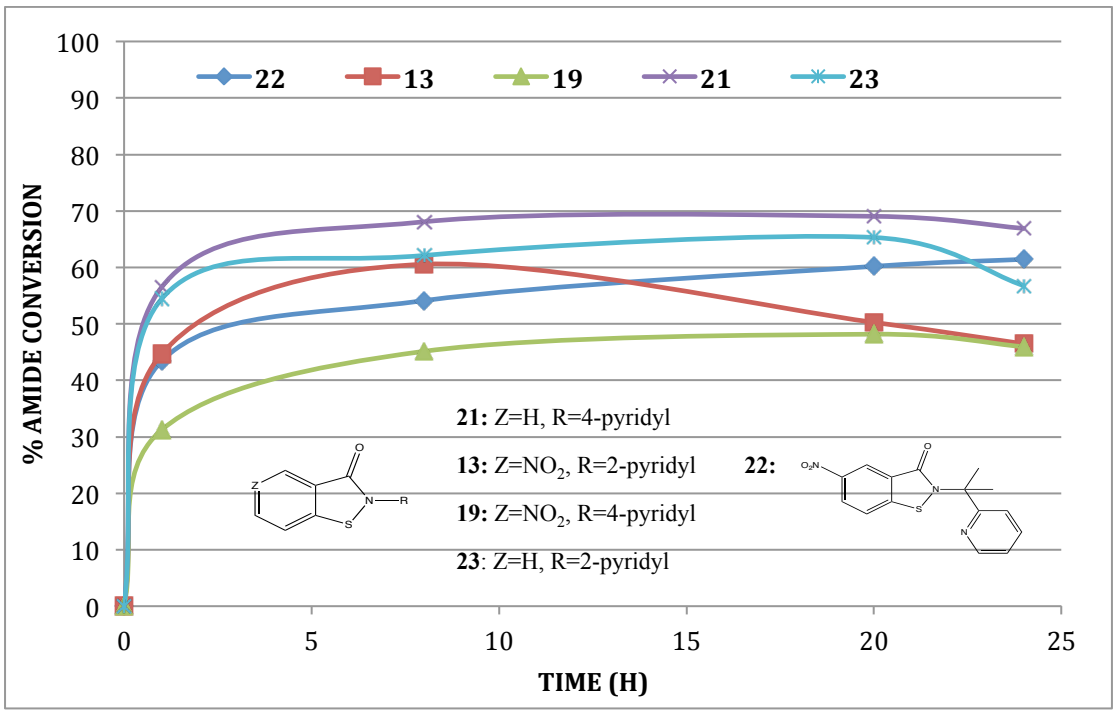

Figure 2. BIT organocatalyst screening in acetonitrile at room temperature over 24 h

Both initial and overall relative catalytic rates differed amongst the BITs depending on the N-substituent and functionalization on the primary aromatic ring. At room temperature, the highest initial and overall rate was observed for **21**, whereas **23** demonstrated the second highest initial rate, and **22** demonstrated the second highest overall catalytic rate.

This experiment was then conducted at 50 ºC with the same BIT organocatalysts in acetonitrile, as shown in Fig. 3.

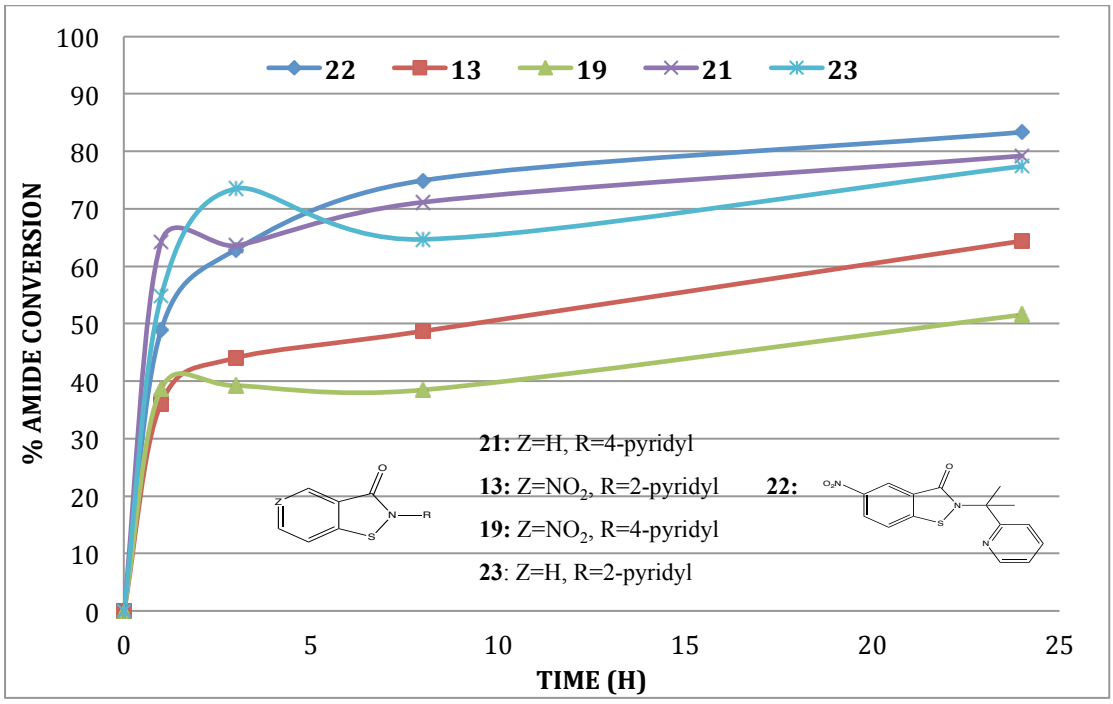

Figure 3. BIT organocatalyst screening in acetonitrile at 50 ºC over 24 h

In comparison to Fig. 2, the % amide conversion in Fig. 3 appear to be increased across all of the tested BITs, affirming the positive correlation between temperature and the catalytic rate. At 50 ºC, however, the best performing BIT was **22**, demonstrating an overall % amide conversion of 83% at the end of the 24-hour time span. BITs **21** and **23** were close behind in terms of catalytic rate and total % amide conversion, with a 79% and 77% conversion respectively.

In both acetonitrile experiments, it can be noted that BITs **13** and **19** consistently demonstrated the worst performance, in terms of total % amide conversion. This low % amide conversion may be attributed to the poor solubility of the nitro-substituted BITs in a large majority of conventional solvents including acetonitrile, DCM, and THF. As the BITs are homogeneous catalysts, any insoluble particles would not contribute to the total catalytic activity; despite standardizing the BIT concentration (20 mol%), the actual concentration of

catalytically active **13** and **19** may have been significantly lower. The insoluble nature of the BITs may be further evidenced by the crystal structure of **13**, as shown in Fig. 4. Crystals of **13** consisted of 2-dimensional sheets of planar molecules closely layering on top of one another, with each layer oriented in such a way that the substituents point in opposite directions. Though the crystal structure of **19** was not obtained, it is likely that it would have resembled Fig. 4 due to the high structural similarities with **13**. The intermolecular attractive forces that exist between these planar structures, as well as the presence of the polar nitro groups may have contributed to the observed insolubility of BITs **13** and **19**.

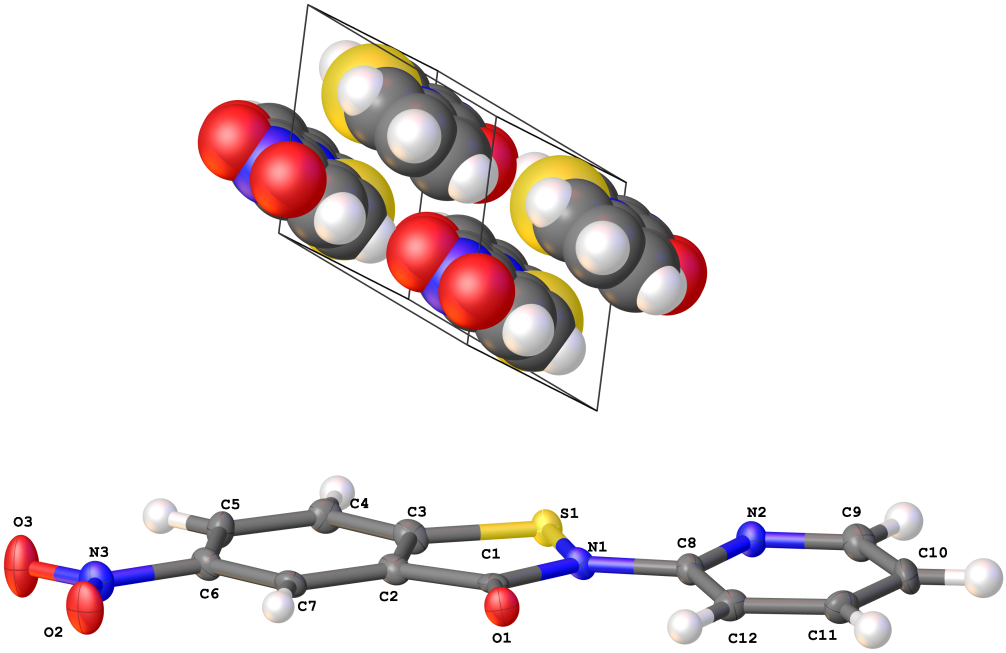

Figure 4. Crystal structure of 5-nitro-2-(pyridin-2-yl)benzo[d]isothiazol-3(2H)-one (**13**)

Insolubilities in the solution may have also interfered with the sampling process. Due to the small volume (15 µL) of each sample, any heterogeneity in amide concentration throughout the reaction vessel could have caused the sample to inaccurately reflect the amide yield at various time points during the reaction.

For **22**, **21,** and **23**, it is possible that a crucial determining factor for the discrepancies in relative catalytic efficiency and overall % amide conversion is the likelihood/rate of the phosphite attack on the sulfur, which initiates S-N bond cleavage as outlined in Scheme 3. At

both room temperature and at 50 ºC, **21** demonstrated a higher amide conversion in comparison to its structural isomer, **23**. As shown in Fig. 5, the pyridyl N in both **21** and **23** can either be protonated by the carboxylic acid or coordinate to the copper complex prior to S-N cleavage. The coordinated copper complex in **23** may exert steric hindrance on the sulfur, preventing efficient phosphite attack to instigate the catalysis process. The pyridyl N in **21**, however, can coordinate with copper in the para position, and the phosphite would be able to approach the sulfur entirely unhindered by the complex. A steric hindrance argument may be proposed for **22** as well; despite the gem-dimethyls creating some distance between the 2-pyridyl N and the sulfur, the phosphite attack would not occur completely unhindered, particularly in comparison to that of **21**. Thus, these discrepancies in the phosphite attack may have contributed to the observed relative catalytic performances of **21**, **22**, and **23** at room temperature—at the lower temperature, where relative rate differences are more significant, the reaction rates may have been sufficiently slow for such kinetic factors to produce a more noticeable effect on the overall catalytic performance of the BITs.

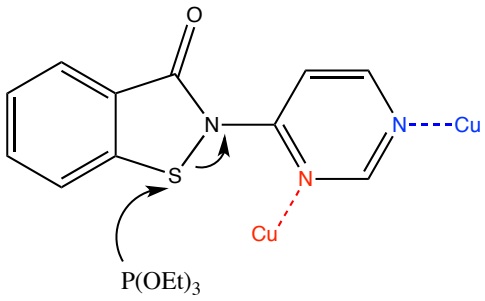

Figure 5. Proposed mechanism of phosphite attack for **23** (red) and **21** (blue)

To further explore the properties of the three best performing BITs, the reaction depicted in Scheme 10 was performed in THF using **21**, **22**, and **23**. Jad et al.[21] identified THF as a suitable solvent in solution-phase peptide bond synthesis, demonstrating high yields comparable to those obtained using acetonitrile. Other than the solvent (previously acetonitrile), all other parameters including the solvent volume were kept constant. The results of the experiments at 50 ºC are demonstrated in Fig. 6.

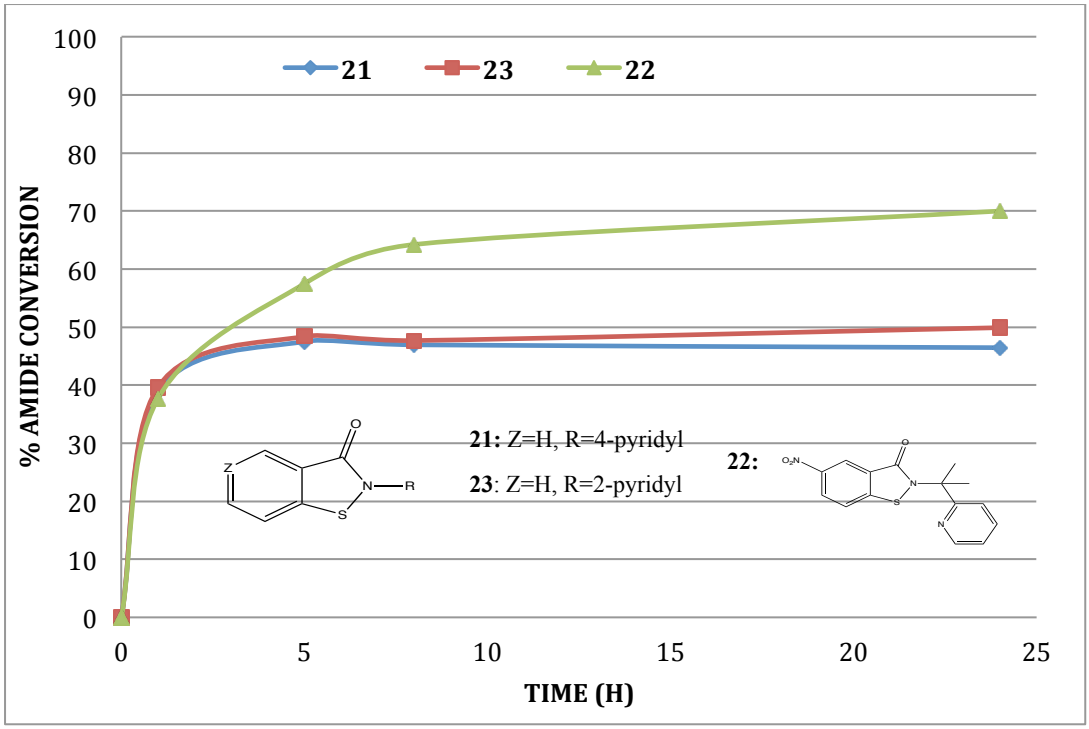

Figure 6. BIT organocatalyst screening in THF at 50 ºC over 24 h

In THF, an overall decline in catalytic performance, both in terms of initial rate and overall % amide conversion, was observed for all of the screened BITs. The extent to which the change in solvent affected performance, however, was not equal amongst the BITs—**21** and **23** experienced an approximately 30% reduction in total % amide conversion whereas **22** was limited to a 13% reduction when compared to the acetonitrile experiments at 50ºC. Maximum % amide conversion was attained at a faster time in THF than in acetonitrile, particularly for **21** and **23**, where reaction rate flat lined by the 5 hour mark.

A likely factor contributing to the reduction in catalytic performance is the unproductive generation and accumulation of the S-ethylation product (**25**) as a result of electrophilic ethoxyphosphonium intermediates, as shown in Scheme 11. Acetonitrile was most likely able to solvate and stabilize the thiolate anion (**24**) more effectively than THF, ultimately resulting in a reduction of the anion's nucleophilicity with respect to the ethoxyphosphonium electrophiles. A slower catalytic inactivation rate would thus increase the lifetime of the BIT, delaying the ultimate plateauing of the reaction rate. Faster

inactivation of the BIT on the other hand would shorten its lifetime and subsequently cause the rate to quickly decline, possibly resulting in the premature flat lining observed in Fig. 5. Further investigation to experimentally quantify the % S-ethylation product over time for the two solvents is imperative to ultimately determine the validity of this scheme.

Scheme 11. Regenerative and inactivating processes

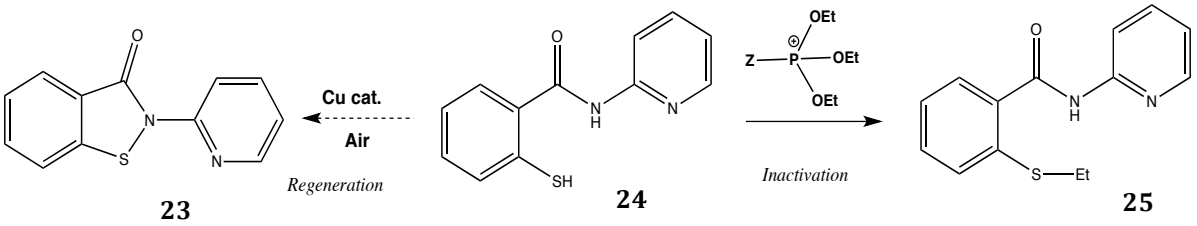

23 **24** **25**

Despite standardization of the sampling protocol for all catalyst-screening experiments, Fig. 2 and 3 demonstrate deviations from the expected exponential curve. Marked decreases in the % amide conversion observed for **13** in Fig. 2 and **23** in Fig. 3 may be attributed either to heterogeneities in the reaction vessel leading to sampling error, or a legitimate degradation of the amide throughout the reaction. Further experiments to confirm the reproducibility of these results would be crucial in the verification of these observations. Other small fluctuations in the catalytic rate that deviate from a smooth curve may be attributed to a general lack of rigorous control over the air pressure at which the reactions took place. Dry air balloons were utilized as a means of providing a steady supply of O_2; however, the precise rate at which oxygen is delivered to the reaction vessel was not quantifiable, and the extent to which the balloons deflated over the course of 24 hours varied slightly from reaction to reaction. With oxygen being the terminal oxidant in the catalytic cycle and therefore an indispensable reagent in the regeneration of the BIT, fluctuations in its supply had a direct impact on the catalytic rate in conjunction with the % amide conversion. To attain the highest level of accuracy in our results, a pressure control system must be established as a means of quantifying and regulating the rate of O_2 delivery across all catalytic reactions.

Conclusions and Future Directions

From this project, it was determined that **21**, **22**, and **23** were the best performing BITs and that using acetonitrile as the solvent optimized their performance. Although this project facilitated a qualitative screening of relative BIT performance, a tighter pressure control system is necessary to obtain a valid, quantitatively accurate comparison of the catalytic rates. Monitoring of other relevant reagents and intermediates in this project, such as the S-ethylation product (**25**), initial *p*-toluic acid, and the deoxygenation dimer of the BIT can also be accomplished on the GC in order to further elucidate the mechanistic information about the catalytic process.

Although in this project, **13** and **19** consistently demonstrated the lowest relative catalytic rates, it was unclear whether these results reflected their true catalytic potential or simply arose due to solubility issues. The solubility of these BITs may be increased by adding some inert functional group (perhaps an isopropyl group) to break the planarity of the structure. A non-planar molecular structure would then liberate the BITs from the observed 2-D sheet structures, enabling enhanced solvation and effectively homogenizing the reaction mixture.

Though our immediate next step is the optimization of the BIT catalytic systems, our long-term goal would be to replace the triethylphosphite reductant with a regenerative alternative that could be coupled with an earth-abundant terminal reductant. A similar catalytic screening and optimization process as that of the catalytic oxidant (and terminal oxidant) would be implemented to develop the catalytic reductant system. By catalyzing both oxidation and reduction processes, we aim to ultimately realize fully catalytic, non-toxic, and Green redox condensation reactions.

Experimental

General Information

Solvents were obtained from Fischer Scientific and dried with JC Mayer solvent drying systems. Ultra-High Purity dry air used in the catalysis studies was purchased from nexAir LLC. Reagents were purchased from Sigma Aldrich, and no subsequent adjustments were made to the purities. Merck silica gel plates were utilized for thin layer chromatography, and phosphorolybdic acid/ninhydrin as well as UV light were used as means to visualize the chromatographs. ^{1}H NMR and ^{13}C NMR spectra were obtained on Varian INOVA 400, VNMR 400, and Mercury 300 spectrometers. Catalysis studies were performed using HP 6850 series GC systems. The Nicolet 380 FT-IR spectrometer was used to collect IR data, with absorption peaks measured in wavenumbers. Compounds were purified using a Biotage flash chromatography system in silica gel flash cartridges. High resolution mass spectra data was obtained from the Emory University Mass Spec Facility, and X-ray crystal structure data was obtained from the Emory University X-ray Crystallography Center. The copper catalyst and BITs **22** and **23**[20] were synthesized by Dr. Pavankumar Gangireddy and were used in the catalysis studies directly as received.

Tert-butyl pyridin-2-ylcarbamate: (10)[24]

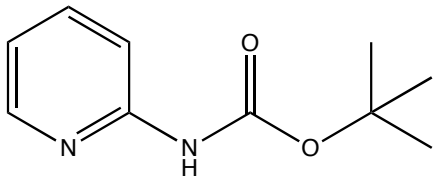

In a flame-dried flask, di*tert*-butyl dicarbonate (9.60 g, 44 mmol, 10.1 mL) was combined with a solution of 2-amino pyridine (3.96 g, 40 mmol) in *tert*-butyl alcohol (65 mL). The mixture was stirred at room temperature (25 ºC) for a period of 24 h. After extracting with

$(C_2H_5)_2O$, the organic layer was dried over $MgSO_4$, and column chromatography was performed on the product. The resulting solution was concentrated *in vacuo* to yield 6.643 g (85 %) of a powdery white solid. ^{1}H NMR (400 MHz, $CDCl_3$) δ 8.56 (s, 1H), 8.29 (dtt, *J* = 4.2, 1.4, 0.9 Hz, 1H), 7.96 (dt, *J* = 8.5, 1.0 Hz, 1H), 7.66 (dddd, *J* = 8.5, 7.2, 1.9, 0.5 Hz, 1H), 6.98 – 6.90 (m, 1H), 1.53 (s, 9H). ^{13}C NMR (101 MHz, $CDCl_3$) δ 152.96, 147.55, 138.30, 117.89, 112.58, 80.67, 28.37, 22.16. IR (neat, cm^{-1}): 1721.09 (s).

2-(*tert*-butylthio)-5-nitrobenzoyl chloride (7)

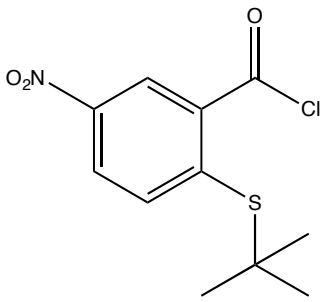

In a flame-dried flask, *tert*-butyl thiol (8.05 g, 89.30 mmol, 8.94 mL) was combined with a solution of 2-chloro-5-nitrobenzoic acid (15 g, 74.42 mmol) in DMF (130 mL). The resulting solution was cooled to 0 ºC, and sodium hydroxide (6.25 g, 156.28 mmol) was added portion wise. The solution was stirred for 8 h, and the progress of the reaction was monitored with thin layer chromatography. After extraction with CH_2Cl_2, the solution was concentrated *in vacuo* to yield 17.1 g (90 %) of a light yellow-green solid. Mp= 176-177 ºC. ^{1}H NMR (400 MHz, DMSO-d_6) δ 13.62 (s, 1H), 8.37 (d, *J* = 2.7 Hz, 1H), 8.23 (dd, *J* = 8.7, 2.7 Hz, 1H), 7.86 (d, *J* = 8.8 Hz, 1H), 1.37 (s, 9H). HRMS (ESI) Calcd. for $C_{11}H_{13}NO_4S$ ($M+H^+$): 256.2902, Found: 256.0638.

2-(*tert*-butylthio)-5-nitrobenzoic acid (3.0 g, 11.75 mmol) was taken up in excess thionyl chloride (13.98 g, 117.51 mmol, 8.52 mL). The mixture was heated to 80 ºC under refluxing conditions for 1h. Completion of the reaction was determined by the transparency of the

resulting yellow solution. The excess $SOCl_2$ was removed through evaporation *in vacuo,* yielding a bright yellow semisolid.

Tert-butyl (2-(_tert_-butylthio)-5-nitrobenzoyl)(pyridin-2-yl)carbamate (11)

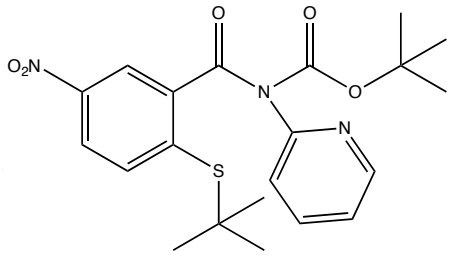

In a flame-dried flask, *tert*-butyl pyridin-2-ylcarbamate (2.0 g, 10.295 mmol) was taken up in dry THF and combined with triethyl amine (1.04 g, 10.295 mmol, 1.43 mL). The mixture was cooled to 0ºC. 2-(*tert*-butylthio)-5-nitrobenzoyl chloride (10.295 mmol) was taken up in dry THF (3-5 mL) and added to the reaction vessel drop-wise. The resulting solution was stirred for 8 h, and completion of the reaction was determined with thin layer chromatography. The reaction was quenched with aqueous sodium bicarbonate. After extraction with CH_2Cl_2, the solution was concentrated *in vacuo* to yield 4.0 g (90 %) of a white semisolid. ^{1}H NMR (400 MHz, $CDCl_3$) δ 8.62 (ddt, J = 4.8, 1.9, 0.6 Hz, 1H), 8.34 – 8.30 (m, 1H), 8.23 – 8.17 (m, 1H), 7.89 – 7.82 (m, 2H), 7.76 – 7.72 (m, 2H), 7.44 (dt, J = 7.9, 1.0 Hz, 1H), 7.37 – 7.32 (m, 2H), 1.38 (s, 9H), 1.18 (s, 9H). ^{13}C NMR (100 MHz, $CDCl_3$) δ 168.82, 151.22, 150.89, 149.48, 147.49, 145.06, 138.37, 138.09, 137.51, 123.64, 123.19, 123.11, 122.38, 84.49, 49.55, 31.60, 27.46. IR (neat, cm^{-1}): 1745 (s), 1687 (s).

2-(*tert*-butylthio)-5-nitro-*N*-(pyridin-2-yl)benzamide (8)

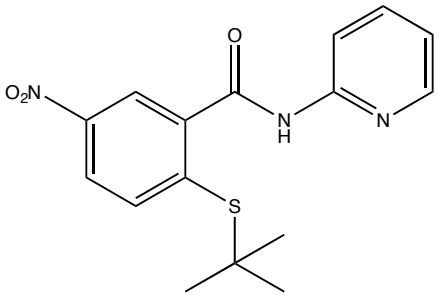

In a flame-dried flask, *tert*-butyl (2-(*tert*-butylthio)-5-nitrobenzoyl)(pyridin-2-yl)carbamate (4.0 g, 9.27 mmol) was taken up in CH_2Cl_2 (15 mL), and the solution was cooled to 0ºC. Trifluoro acetic acid (24.098 g, 211.36 mmol, 17 mL) was added to the reaction vessel drop wise. The mixture was stirred for 8 h, and completion of the reaction was determined with thin layer chromatography. The reaction was quenched with aqueous sodium bicarbonate until a neutral pH was attained. After extraction with CH_2Cl_2, the solution was concentrated *in vacuo* to yield 2.7422 g (90 %) of a yellow solid. ^{1}H NMR (400 MHz, $CDCl_3$) δ 10.29 (s, 1H), 8.89 (q, J = 2.1, 1.3 Hz, 1H), 8.33 (d, J = 8.4 Hz, 1H), 8.30 – 8.21 (m, 2H), 7.84 – 7.71 (m, 2H), 7.07 (ddt, J = 7.7, 4.5, 1.4 Hz, 1H), 1.34 (s, 9H). ^{13}C NMR (100 MHz, $CDCl_3$) δ 163.98, 151.18, 147.90, 147.77, 141.62, 139.63, 138.65, 138.58, 125.16, 124.36, 120.26, 114.73, 50.38, 31.00. IR (neat, cm^{-1}): 1684. HRMS (ESI) Calcd. for $C_{16}H_{17}N_3O_3S$ ($M+H^+$): 332.0991, Found: 332.1055.

5-nitro-2-(pyridin-2-yl)benzo[*d*]isothiazol-3(2*H*)-one (13)

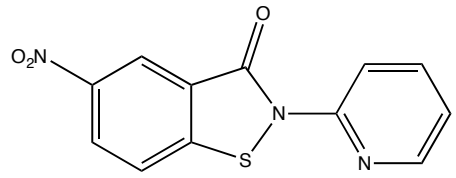

In a flame-dried flask, 2-(*tert*-butylthio)-5-nitro-*N*-(pyridin-2-yl)benzamide (0.200 g, 0.60 mmol) was taken up in 0.2 M CH_2Cl_2 and cooled to 0º C. 3-Chloroperoxybenzoic acid (0.104 g, 0.60 mmol) was added to the reaction vessel portion wise. The reaction was monitored with thin layer chromatography. Upon formation of the product, the reaction was immediately quenched by addition of aqueous sodium bicarbonate solution. The reaction mixture was extracted with CH_2Cl_2, dried over $MgSO_4$, and concentrated *in vacuo*. The resulting solid was taken up in toluene (5 mL) and heated while the reaction was monitored by TLC. After complete conversion to the product, excess toluene was removed *in vacuo* to yield 0.1226 g (74%) of bright greenish yellow solid. Mp= 282-284 ºC. ^{1}H NMR (400 MHz, $CDCl_3$) δ 8.91 (dd, *J* = 2.3, 0.6 Hz, 1H), 8.69 (dt, *J* = 8.4, 1.0 Hz, 1H), 8.48 (ddd, *J* = 8.7, 2.2, 0.4 Hz, 1H), 8.41 (ddd, *J* = 5.0, 1.8, 0.9 Hz, 1H), 7.88 – 7.80 (m, 1H), 7.74 (dd, *J* = 8.8, 0.6 Hz, 1H), 7.22 – 7.17 (m, 1H). IR (neat, cm^{-1}): 1660 (s). HRMS (ESI) Calcd. for $C_{12}H_7N_3O_3S$ ($M+H^+$): 274.0208, Found: 274.02757.

2-(*tert*-butylthio)-5-nitro-*N*-(pyridin-4-yl)benzamide (17)

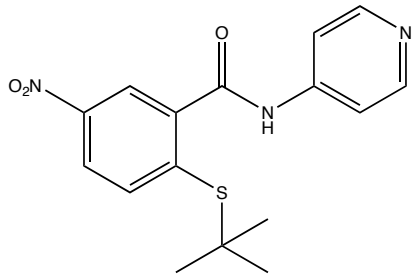

In a flame-dried flask, 4-amino pyridine (0.55 g, 5.877 mmol) was taken up in 0.1 M dry THF (20 mL) and cooled to 0 ºC. 2-(*tert*-butylthio)-5-nitrobenzoyl chloride (1.959 mmol) was taken up in dry THF (10 mL) and added to the reaction vessel drop-wise. The resulting solution was stirred for 8 h, and completion of the reaction was determined with thin layer chromatography. The reaction was quenched with aqueous sodium bicarbonate. After extraction with CH_2Cl_2, the solution was concentrated *in vacuo* to yield 0.4993 g (77 %) of a yellow solid. ^{1}H NMR (400 MHz, $CDCl_3$) δ 10.34 (s, 1H), 9.01 (d, J = 2.6 Hz, 1H), 8.60 – 8.53 (m, 2H), 8.28 (dd, J = 8.4, 2.7 Hz, 1H), 7.82 (dd, J = 8.4, 0.4 Hz, 1H), 7.65 – 7.58 (m, 2H), 1.33 (s, 9H). ^{13}C NMR (100 MHz, $CDCl_3$) δ 163.70, 150.89, 148.44, 144.41, 140.64, 140.53, 137.23, 126.26, 124.96, 113.93, 51.20, 30.88.

5-nitro-2-(pyridin-4-yl)benzo[*d*]isothiazol-3(2*H*)-one (19)

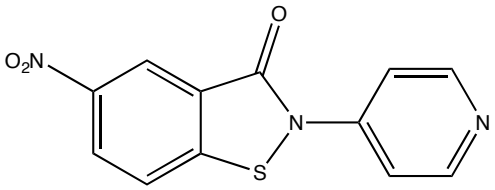

This compound was prepared using the same protocol as **13** by first using 2-(*tert*-butylthio)-5-nitro-*N*-(pyridin-4-yl)benzamide (**17**) and 3-chloroperoxybenzoic acid. The resulting compound heated in toluene and monitored with TLC. The solution was concentrated *in vacuo* to yield 0.184 g (56%) of a bright yellow solid. Mp= 274-276 ºC. ^{1}H NMR (400 MHz, $CDCl_3$) δ 8.95 (dd, J = 2.2, 0.6 Hz, 1H), 8.74 – 8.67 (m, 2H), 8.55 (dd, J = 8.8, 2.3 Hz, 1H),

7.84 – 7.74 (m, 3H). IR (neat, cm^{-1}): 1676 (s). HRMS (ESI) Calcd. for $C_{12}H_7N_3O_3S$ ($M+H^+$): 274.0208, Found: 274.0280.

2-(methylthio)benzoyl chloride (20)[23]

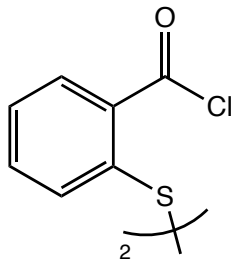

In a flame-dried flask, 2-(methylthio)benzoic acid (10.0 g, 32.64 mmol) was taken up in excess $SOCl_2$ (38.83 g, 326.41 mmol, 23.68 mL). The mixture was heated to 80ºC under refluxing conditions for 8h. Completion of the reaction was determined by the formation of a clear dark brown solution. The excess $SOCl_2$ was removed through evaporation *in vacuo,* yielding a dark brown solid.

2-(pyridin-4-yl)benzo[*d*]isothiazol-3(2*H*)-one (21)[22]

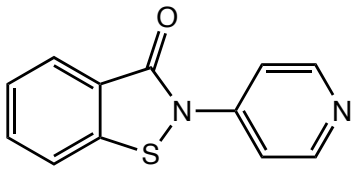

In a flame-dried flask, 4-amino pyridine (0.685 g, 7.284 mmol) was taken up in 0.1 M dry THF and cooled to 0ºC. 2-(methylthio)benzoyl chloride (0.500 g, 1.46 mmol) was taken up in dry THF (5 mL) and added to the reaction vessel drop-wise. The resulting solution was stirred for 8 h., and completion of the reaction was determined with thin layer chromatography. The reaction was quenched by addition of aqueous sodium bicarbonate. After extraction with CH_2Cl_2, the organic layer was dried over $MgSO_4$ and a TLC was obtained. Column chromatography was performed on the compound, and the resulting

solution was concentrated *in vacuo* to yield 0.262 g (32.7%) of a white solid. Mp= 184-185 ºC. ^{1}H NMR (400 MHz, $CDCl_3$) δ 8.95 (dd, *J* = 2.2, 0.6 Hz, 1H), 8.74 – 8.67 (m, 2H), 8.62 – 8.51 (m, 1H), 7.84 – 7.74 (m, 3H). ^{13}C NMR (100 MHz, $CDCl_3$) δ 164.51, 150.97, 144.99, 138.98, 133.29, 127.38, 126.24, 124.80, 120.15, 115.76. IR (neat, cm^{-1}): 1660 (s).

Benzoisothiazolone Screening Studies:

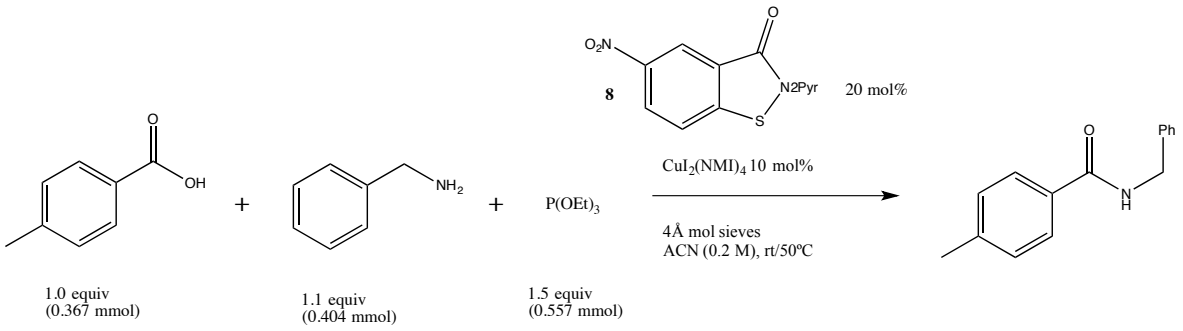

185 mg of 4 Å molecular sieves were activated in the microwave for four minutes in 12 mL test tubes. In each test tube, BIT (0.073 mmol, 0.2 equiv), *p*-toluic acid (50 mg, 0.367 mmol), 1,3,5 tri-tertbutylbenzene (91 mg, 0.367 mmol, 1 equiv), and $CuI_2(NMI)_4$ (23.72 mg, 0.037 mmol, 0.1 equiv.) were combined and taken up in 0.2 M acetonitrile (1836 µL). $P(OEt)_3$ (92 mg, 0.557 mmol, 1.5 equiv, 94 µL) and phenyl methanamine (43.3 mg, 0.404 mmol, 1.1 equiv, 44.1µL) were added to the mixture. Each BIT experiment was commenced at staggered times in order to avoid sampling at the same time. The reaction was stirred and put under dry air using air balloons. 15 µL samples of each mixture was taken at 1 h, 3 h, 5 h, 8 h, 20 h, and 24 h and quenched with 150 µL of THF. Amide conversion percentage was determined by gas chromatography, for which several microliters of the samples were used.

GC Parameters:

Column: Agilent HP-5, length -30 m, diameter 0.32 mm, film 0.25 µm

Method: Initial temp: 70 ºC (0 min), ramp: ºC/min to 320 ºC (7 minute wait time, 19.0 minutes total time)

References

[1] Mukaiyama, T. Oxidation-reduction condensation a new method for peptide synthesis. *Synth. Commun.* **1971**, *2*(5), 243-265.

[2] Mukaiyama, T. Oxidation-reduction condensation. *Angew. Chem. Int. Ed.* **1976**, *15*, 94-103.

[3] But, T. Y.; Toy, P. H. The Mitsunobu reaction: origin, mechanism, improvements, and applications. *Chemistry, an Asian journal* **2007**, *2*, 1340-1355.

[4] Mukaiyama, T.; Shintou, T.; Fukumoto, K. A convenient method for the preparation of inverted tert-alkyl carboxylates from chiral tert-alcohols by a new type of oxidation-reduction condensation using 2,6-dimethyl-1,4-benzoquinone. *J. Am. Chem. Soc.,* **2003,** *125*(35), 10538-10539.

[5] Mukaiyama, T.; Kuroda, K.; Maruyama, Y. A new type of oxidation-reduction condensation by the combined use of phenyl diphenylphosphinite and oxidant. *Heterocycles* **2010**, *80*, 63.

[6] Hughes, D. *Organic Reactions* **1992**, *42*, 335-656.

[7] Luo, Q.; Lv, L.; Li, Y.; Tan, J.; Nan, W.; Hui, Q. An efficient protocol for the amidation of carboxylic acids promoted by trimethyl phosphite and iodine. *Eur. J. Org.Chem.* **2011**, *2011*(34), 6916-6922.

[8] Mukaiyama, T. Explorations into new reaction chemistry. Angew. *Chem. Int. Ed.* **2004**, *43*, 5590-5614.

[9] Swamy, K. C.; Kumar, N. N.; Balaraman, E.; Kumar, K. V. P. Mitsunobu and related reactions: advances and applications. *Chem. Rev.* **2009**, *109*(6), 2551-2651.

[10] Ahn, C.; Correia, R.; DeShong, P. Mechanistic study of the Mitsunobu reaction. *J. Org. Chem.* **2002**, *67*(6), 1751-1753.

[11] Constable, D. J.; Dunn, P. J.; Hayler J. D.; Humphrey, G. R.; Leazer, J. L.; Linderman, R. J.; Lorenz, K.; Manley, J.; Pearlman, B.; Wells, A.; Zaks, A.; Zhang, T. Key green chemistry research areas—a perspective from pharmaceutical manufacturers. *Green Chem.* **2007**, *9*, 411-420.

[12] Santa Cruz Biotechnology. "Material safety data sheet: diethyl azodicarboxylate". http://datasheets.scbt.com/sc-280673.pdf (accessed Mar 25, 2016).

[13] But, T. Y.; Toy, P. H. Organocatalytic Mitsunobu reactions. *J. Am. Chem. Soc.* **2006**, *128*, 9636-9637.

[14] Hirose, D.; Taniguchi, T.; Ishibashi, H. Recyclable Mitsunobu reagents: catalytic Mitusnobu reactions with an iron catalyst and atmospheric oxygen. *Angew. Chem. Int. Ed.* **2013**, *52*, 4613 -4617.

[15] Ueki, M.; Maruyama, H.; Mukaiyama, T. Peptide synthesis by oxidation-reduction condensation. I. Use of NPS-peptides as amino component. *Bull. Chem. Soc. Jpn.* **1971**, *44*, 1108-1111

[16] Villalobos, J. M. PhD, Emory University, 2007.

[17] Wang, Z.; Kuninobu, Y.; Kanai, M. Copper-catalyzed intramolecular N-S bond formation by oxidative dehydrogenative cyclization. **2013**, *78*, 7337-7342.

[18] Lanny S. Liebeskind and Pavankumar Gangireddy, unpublished results.

[19] Goodgame, D. M. L.; Goodgame, M.; Rayner-Canham, G. W. *Inorg. Chim. Acta* **1969**, *3*, 406-410.

[20] Kamigata, N.; Iizuka, H.; Kobayashi, M. *Bull. Chem. Soc. Jpn.* **1986**, 59.

[21] Jad, Y.; Acosta, G.; Khattab, S.; de la Torre, B.; Govender, T.; Kruger, H.; El-Faham, A.; Albericio, F. Peptide synthesis beyond DMF: THF and ACN as excellent and friendlier alternatives. *Org. Biomol. Chem.* **2015**, *13*(8), 2393-2398.

[22] Terauchi, H.; Tanitame, A.; Tada, K.; Nishikawa, Y. A convenient synthesis of N-substituted 2,3-dihydro-3-oxoisothizaolo[5,4-b]pyridines in acidic conditions. *Heterocycles.* **1996**, *43*(8), 1719-1734.

[23] Zhai, L.; Guo, L.; Luo, Y.; Ling, Y.; Sun, B. Effective laboratory-scale preparation of axitinib by two CuI-catalyzed coupling reactions. *Org. Process Res. Dev.* **2015**, *19*, 849-857.

[24] Zeng, J.; Tan, Y.; Leow, M.; Liu, X. Copper(II)/Iron(III) co-catalyzed intermolecular diamination of alkynes: facile synthesis of imidazopyridines. *Org. Lett.*, **2012**, *14*(17), 4386-4389.